

Realizing Ultralow Concentration Gelation of Graphene Oxide with Artificial Interfaces

Chong Luo, Wei Lv,* Changsheng Qi, Lixiang Zhong, Zheng-Ze Pan, Jia Li,* Feiyu Kang, and Quan-Hong Yang*

Understanding the chemistry in the gelation (interfacial assembly) of graphene oxide (GO) is very essential for the practical uses of graphene-based materials. Herein, with the designed artificial interfaces due to the introduction of water-miscible isopropanol, the gelation of GO is achieved in water at an ultralow concentration (0.1 mg mL^{-1} , the lowest ever-reported) with a solvothermal treatment. Intrinsically, with a lower intercalation energy, water shows much stronger attraction with GO than isopropanol, inducing a microphase separation in the miscible mixture of isopropanol and water. In the solvothermal process, the partially reduced GO sheets interact with each other along the water–isopropanol interface and assemble into interconnected frameworks. In general, the formation of the artificial interface results in locally concentrated GO in the water phase, which is the final driving force for the gelation at ultralow concentration. Thus, the threshold for the GO gelation concentration is dependent upon the water fraction in the mixture and water acts as the spacer to facilitate the gelation and final control of the resulting materials microstructure. This study enriches interface/gelation chemistry of GO and indicates a practical way for precise structural control and scale-up preparation of graphene-based materials.

The hydrogels of graphene oxide (GO) and reduced graphene oxide (r-GO) have drawn significant attention because they not only inherit the structural advantages and unique properties

of graphene but also show high surface utilization and easy processability.^[1–6] These advantages make them more applicable than individual graphene sheets in many cases, including energy storage, environmental protection, and biomedical-related systems, etc.^[7–14] Hydrothermal or solvothermal treatment, starting from GO solution, are commonly used for the synthesis of GO hydrogels.^[15–19] Our previous paper had reviewed and discussed the key factors for such gelation processes, such as the solvent properties, the concentrations of the suspension, and the surface chemistry of GO.^[3] Solvothermal or hydrothermal reduction is an important approach to initiate the assembly of GO in solution. The partially removed oxygen-containing hydrophilic groups result in a relatively increased π – π attraction and trigger the interaction between r-GO sheets to assemble into various structures.^[20,21]


A review of the reported results illustrated that a relatively high GO concentration (normally higher than 1 mg mL^{-1} , Table S1, Supporting Information) was needed to ensure the formation of hydrogels, otherwise only the precipitate is obtained due to less possibility of overlapping.^[3,16,22] Moreover, it is also difficult to precisely control the microstructure of hydrogels due to the unclear gelation process, hindering the mass production, and extended applications. The GO gelation at low concentration is hard to achieve and lack of investigation. However, the GO concentration should not be the prerequisite for GO assembly, where low concentration gelation should be able to realize through increasing the GO interactions at interfaces. Thus, a deep understanding of the gelation process at low concentration and its mechanism is urgently required.

In this study, we report an unexpected finding that at an ultralow GO concentration (as low as $\approx 0.1 \text{ mg mL}^{-1}$), gelation still occurs and a hydrogel monolith is formed in a water–isopropanol mixture through a solvothermal treatment. To the best of our knowledge, this is the lowest concentration ever found to initiate the formation of macroscale GO hydrogels, which is an order of magnitude lower than the previous results. The key factor here is the utilization of water–isopropanol mixture rather than pure water in the solvothermal process. Thus, a high GO concentration is not the precondition for hydrogel formation and an in-depth analysis

C. Luo, Prof. W. Lv, Z.-Z. Pan
Shenzhen Geim Graphene Center
Engineering Laboratory for Functionalized Carbon Materials
Graduate School at Shenzhen
Tsinghua University
Shenzhen 518055, China
E-mail: lv.wei@sz.tsinghua.edu.cn

C. Qi, Prof. Q.-H. Yang
Nanoyang Group
State Key Laboratory of Chemical Engineering
School of Chemical Engineering and Technology
Tianjin University
Tianjin 300072, China
E-mail: qhyangcn@tju.edu.cn

L. Zhong, Prof. J. Li, Prof. F. Kang
Key Laboratory of Thermal Management Engineering and Materials
Graduate School at Shenzhen
Tsinghua University
Shenzhen 518055, China
E-mail: lijia@phys.tsinghua.edu.cn

 The ORCID identification number(s) for the author(s) of this article can be found under <https://doi.org/10.1002/adma.201805075>.

DOI: 10.1002/adma.201805075

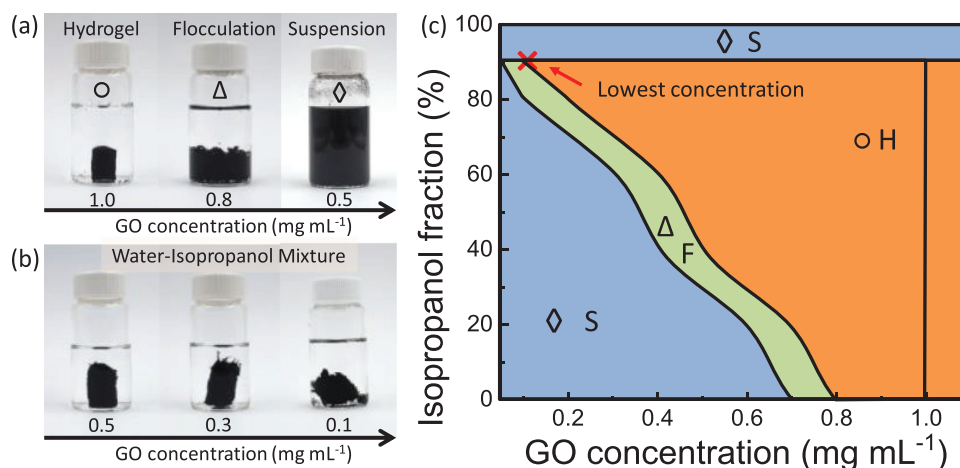


Figure 1. a) Typical photos of r-GO hydrogel, flocculation, and suspension obtained from GO aqueous solution at different concentration; b) the photos of r-GO hydrogels synthesized in water–isopropanol mixture at different GO concentration; c) the phase diagram of diverse r-GO configurations after solvothermal process at different GO concentration versus isopropanol fraction, where the orange, green, and blue regions represent hydrogel (○ H), flocculation (△ F), and suspension (◇ S), respectively.

demonstrates that the intrinsic solvent properties are mainly responsible for the initiation of the gelation process. More importantly, due to the different attractions between GO and two different solvents, the microphase separation of the mixed solvent is detected, inducing GO sheets gradually precipitate and assemble along the liquid–liquid microinterfaces. Such interfaces were generated by the artificially adding secondary solvent and were denoted as artificial interfaces. In this system, the fraction of water is found to play a crucial role not only in promoting the gelation but also in determining the formation of the pore structure. Hence, the structure of the hydrogels can be easily and effectively tuned by changing the water fraction. Such a gelation process is important for the better understanding of the assembly mechanism of GO and facilitates the development of advanced graphene-based materials in practical applications.

Typically, the GO hydrogels can be easily prepared from an aqueous solution through a hydrothermal treatment. As shown in Figure 1a and Figure S1 in the Supporting Information, GOs with different concentrations can assemble into diverse r-GO configurations with exactly the same hydrothermal treatments. A regular-shaped r-GO monolith can be formed when the GO concentration is above 1 mg mL⁻¹. GOs just flocculate at lower concentration (0.8 mg mL⁻¹) and do not form integral macroscale monolith. At a lower concentration (0.5 mg mL⁻¹), only an r-GO suspension can be obtained, ascribing to the lower possibility of the interaction or overlapping between GO sheets. In a sharp contrast, as shown in Figure 1b, we found that an integral GO hydrogel can be formed at 0.5 mg mL⁻¹ when a small fraction of water is mixed with isopropanol. In the water–isopropanol mixture, the r-GO monolith can still be obtained even at a lower GO concentration (0.3 mg mL⁻¹) through tuning the fraction of isopropanol in the mixture. The lowest concentration for the r-GO hydrogel formation can even reach as low as 0.1 mg mL⁻¹, which is an order of magnitude lower than those in previous reports. Above results demonstrate that with a suitable GO concentration and water fraction, GO gelation will still occur and an integral r-GO hydrogel can be obtained in the water–isopropanol mixture. In order to

further illustrate the relationship between GO concentration and solvent fraction, a series of systematical experiments were conducted and a phase diagram was summarized in Figure 1c. The three different color regions, orange, green, and blue, respectively, represent different r-GO configurations, hydrogel (○ H), flocculation (△ F), and suspension (◇ S), forming at different GO concentrations or isopropanol fractions. The r-GO hydrogels in orange region should have physical integrity with definite shape and mechanical strength with cross-linked long-range network. The typical r-GO hydrogel should present higher storage modulus G' than the loss modulus G'' at all measured frequency as shown in Figure S2 in the Supporting Information. However, due to no long-range cross-linked network, r-GO suspension shows more liquid-like behavior, where the loss modulus G'' will cross over at higher frequency. The suspension in the blue region represents GO sheets temporarily dispersed in pure isopropanol and will eventually precipitate. The phase diagram presents an effective guideline to design the experimental formula and predicts the GO concentration threshold in each isopropanol fraction. Interestingly, a linear relationship (Figure S3, Supporting Information) was obtained between the threshold GO concentration and water fraction. The constant slope can be regarded as the threshold concentration of GO in the water phase among the mixture, where above concentration guarantees the sufficient interactions and the assembly of GO sheets. And the achieved lowest GO concentration for forming an integral GO hydrogel is as low as 0.1 mg mL⁻¹ (90 vol% isopropanol). The significant differences of GO configurations observed after the solvothermal process indicate the solvent property is the key factor for GO gelation at low concentrations.

Figure 2 illustrates the interaction between GO sheets and different solvents. Due to the oxygen-containing groups, GO sheets are hydrophilic and can well dissolve in water, forming a stable dispersion as shown in Figure 2a. However, the isopropanol is a poor solvent for GO and unable to form a stable dispersion, which will precipitate after several hours. Therefore, in order to form a stable GO dispersion in the water–isopropanol

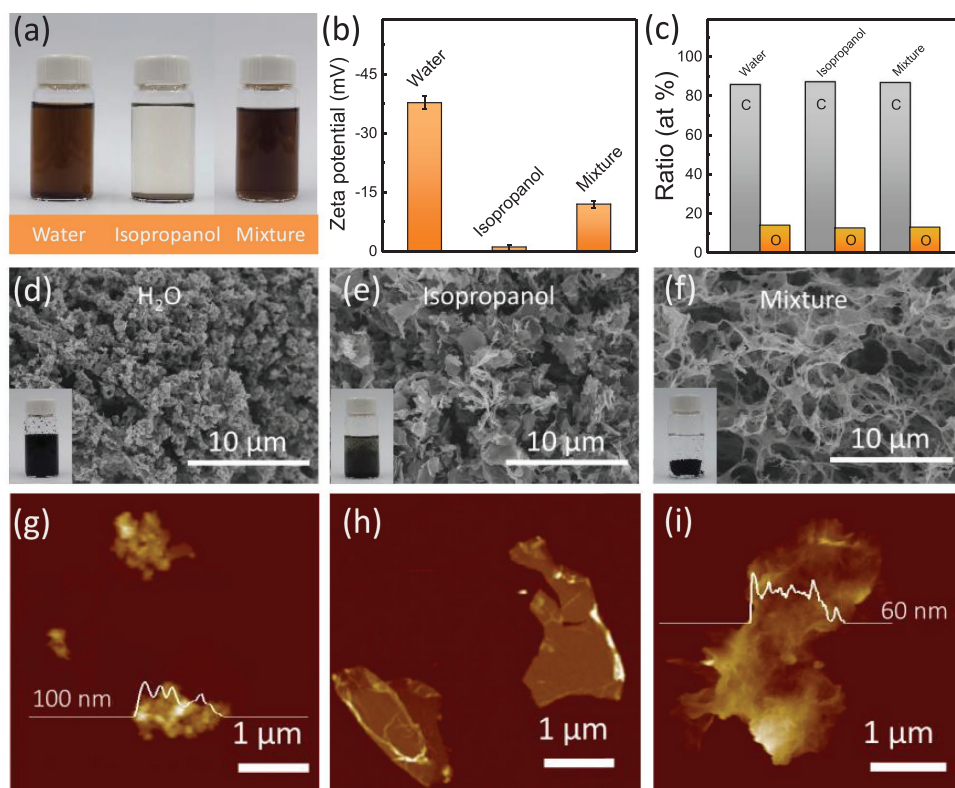


Figure 2. a) The photo of GO dispersion in water, isopropanol, and water–isopropanol mixture (0.4 mg mL^{-1}); b) zeta potentials of these dispersion; c) the carbon/oxygen atom ratios of these freeze-dried r-GO products after the solvothermal treatment; d–f) SEM and g–i) AFM images of freeze-dried r-GO products, inset are the photos of these r-GO products before freeze-drying.

mixture, a GO aqueous solution is required to be prepared first and then diluted by the isopropanol. The zeta potential measurement in Figure 2b further demonstrates the different stability of these solvents. GO in water has much stronger electrostatic repulsion than those in isopropanol and the mixture, which can, therefore, maintain the stable solution. These indicate that GO sheets have stronger attractions with water molecules than with isopropanol, where GO sheet surface prefers to be hydrated first and then surrounded by isopropanol molecules. The GO sheets' arrangement in these solutions was directly observed under the cross-polarizers in Figure S4 in the Supporting Information. The GO aqueous solution presents uniform-ordered nematic phase and water–isopropanol mixture exhibited more isotropic phase with less alignment. These demonstrated that the introduced isopropanol smashed the ordered alignment of pristine GO sheets and generated more microinterfaces in the mixture, facilitating the interaction and assembly of GO sheets.

With the solvothermal process, the r-GO products have the similar reduction degree in different solvents, as proven by the similar carbon/oxygen atom ratios from the X-ray photoelectron spectroscopy (XPS) spectra (Figure 2c and Figure S5, Supporting Information) and the similar bonding in C1s XPS spectra (Figure S6, Supporting Information). The similar UV–Vis spectra (Figure S7, Supporting Information), Fourier-transform infrared spectroscopy (FT-IR) spectra (Figure S8, Supporting Information), and I_D/I_G ratios (1.04–1.08) in the Raman spectra (Figure S9, Supporting

Information) also confirmed the similar reduction level and no reactions between GO and solvents, where the additional peaks of C–H may ascribe to some remained solvents in the sample.^[23] The microstructures of r-GO products through different solvothermal treatments in pure water, isopropanol, and their mixtures were examined after freeze-drying by a scanning electron microscope (SEM). The freeze-dried r-GO sheets obtained in pure water (Figure 2d) are severely aggregated and crumpled, which is further confirmed by the atomic force microscope (AFM) images shown in Figure 2g. These results also indicate that the GO sheets tend to crumple but cannot be fully interconnected forming a network with a low concentration. In contrast, the freeze-dried r-GO sheets precipitated from isopropanol are flat with a large lateral size and uniform thickness (Figure 2e,h) due to the poor dispersibility and less interaction between GO and isopropanol.^[24] A well-developed interconnected 3D porous r-GO network is formed in the water–isopropanol mixture (Figure 2f). Even after a strong sonication pretreatment for AFM characterization, the 3D micro-scale network is still clearly identified (Figure 2i). These results demonstrate that the GO sheets in water–isopropanol mixture tend to interact with each other even at a very low GO concentration. According to the previous discussion, the hydrated GO sheets may generate a microphase separation from isopropanol molecules, inducing micro liquid–liquid interfaces for interaction and nucleation of r-GO sheets. Then the separated water phase may serve as the spacer to avoid the parallel overlapping and form the interlinked network.

Other solvents with different properties were selected as the secondary components in the mixture to testify the above discussion. Similar experiments were performed using secondary solvents mixed with water (20 vol%) at a low GO concentration (0.4 mg mL^{-1}). The first three monohydric alcohols (methanol, ethanol, and isopropanol), one hydroxyl and water-miscible, can form an integral r-GO hydrogel. However, butanol has poor water solubility and lower density, which will separate from the GO aqueous phase. During the solvothermal process, the amphiphilic GO sheets are gradually reduced into hydrophobic r-GO and transfer from the water phase into the butanol phase. Due to phase separation, no water serves as the spacer to prevent the parallel restacking and only r-GO sediment can be obtained. These results demonstrate a water-miscible secondary solvent is required to hold the water as the spacer and form the connected network.

Ethylene glycol (EG) has two hydroxyls and stronger hydrogen bonding compared with the previous alcohols, which has better dispersibility for GO sheets. *N,N*-dimethylformamide (DMF) is also a widely used good solvent for dispersing GO and r-GO sheets. GO sheets can be homogeneously dispersed in these solvent–water mixtures without locally concentrated phase, which is short of the interfaces to trigger the interaction and gelation at low concentration. Therefore, no hydrogel is formed and only flocculation (EG) or suspension (DMF) can be obtained. Due to the better dispersibility with r-GO, products in DMF can form a suspension instead of the flocculation. Based on the above results, good solvents for GO (like EG and DMF) have strong attractions with GO sheets, resulting in a lack of concentrated phase and interfaces to assemble r-GO sheets. Therefore, the solvents that are not good for dispersing GO (such as methanol, ethanol and isopropanol) are selected to mix with water to ensure the gelation and form integral hydrogels at low concentrations.

In order to further support our speculation, density functional theory (DFT) calculations were performed to demonstrate the intercalation energies and predict which solvent prefers to accumulate between r-GO sheets. The intercalation energy difference of these solvents may lead to the microphase separation and the formation of spacers facilitating the assembly

process. In order to evaluate the stability of molecule intercalation, we considered the solvent molecules intercalate into a double-layer graphene (DLG) decorated with oxygen-containing groups. The intercalation energies (E_c) of solvent molecules in GO are defined by Equation (1)

$$E_c = E_{\text{tot}} - E_0 - E_m \quad (1)$$

where E_{tot} and E_0 are the total energies of the GO with and without solvent molecule intercalation, respectively, and E_m is the energy of a solvent molecule. As discussed above, the r-GO still contains some oxygen-containing groups, i.e., epoxy and hydroxyl groups, which decorate on the graphene sheets and have an influence on the intercalation energy.^[23,25] As shown in Figure S10 in the Supporting Information, we calculated the E_c of a water molecule and an isopropanol molecule in DLG and DLG with two epoxy (DLG-2O) or hydroxyl (DLG-2OH) groups on opposing graphene sheets. The results indicate that the solvent molecules are easier to intercalate into the DLG-containing functional groups compared with DLG. The water molecule requires less energy (0.04 eV) than an isopropanol molecule (0.35 eV) to be stabilized between the DLG-2OH sheets. Thus, water has more attraction and interaction with GO sheets compared with isopropanol, which is ascribed to the higher polarity and hydrogen bonds. Other solvents, like EG and DMF, were also calculated to demonstrate their interaction with DLG-2OH sheets (Figure 3b). The lower energies for EG (−0.04 eV) and DMF (−0.21 eV) indicated that they have stronger interaction between GO sheets compared with water, which is consistent with previous results and only a suspension or flocculation can be obtained. Other combinations, like EG/isopropanol or DMF/isopropanol (Figure S11, Supporting Information), with larger intercalation energy differences can also form r-GO hydrogels at low concentration. Therefore, the secondary solvent should have higher intercalation energy than the previous solvent, where GO sheets prefer to accumulate around one phase and generate micro liquid–liquid interfaces facilitating the assembly of r-GO hydrogels. This is consistent with the above results and water-miscible GO poor solvents are chosen for the gelation at low concentration.

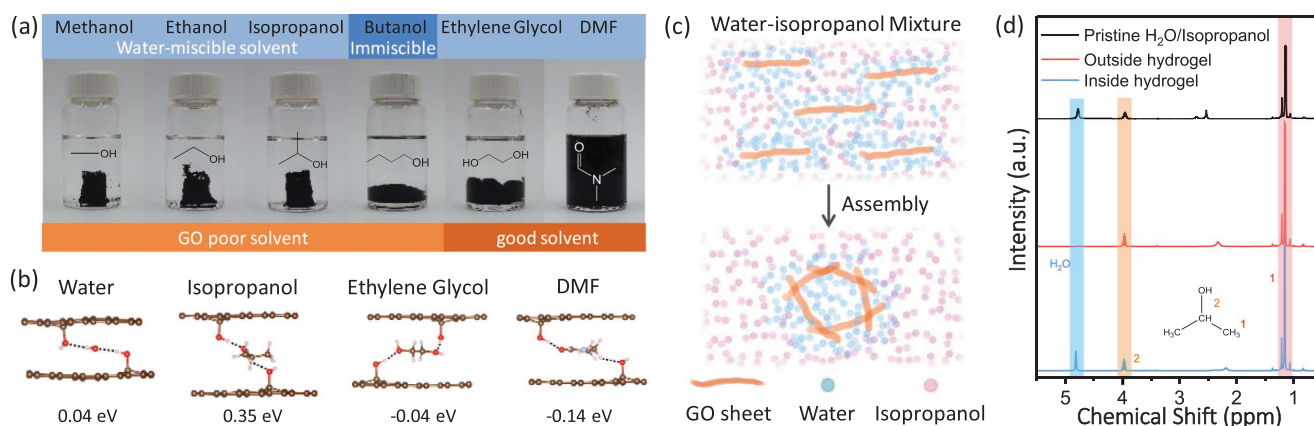


Figure 3. a) The r-GO products in different solvents–water mixtures after solvothermal treatment (from left to right: methanol, ethanol, isopropanol, butanol, ethylene glycol and DMF); b) calculation models and intercalation energies of solvent molecules (water, isopropanol, EG, and DMF) intercalated in DLG-2OH; c) schematic diagram illustrates the microphase separation and the distribution of GO sheets and solvent molecules in the dispersion; d) the NMR spectra of the liquids in different regions among the water–isopropanol mixture.

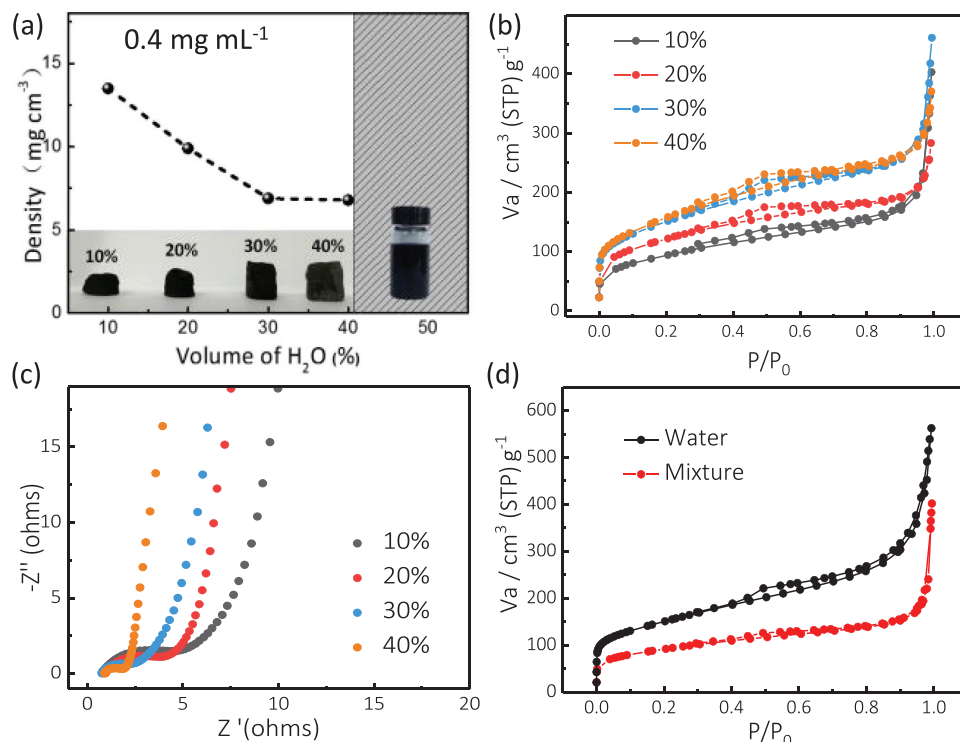


Figure 4. a) Photos and density of aerogels obtained with different water fractions at a fixed GO concentration of 0.4 mg mL^{-1} ; b) N_2 adsorption isotherms and c) Nyquist plots of r-GO aerogels; d) N_2 adsorption isotherms of high GO concentration aerogels obtained in aqueous solution or water-isopropanol mixture.

Although alcohols are water-miscible, in molecule level alcohols and water are not completely mixed and alcohols can form aggregates hiding hydrophobic groups, which may induce microphase separation in some specific environment.^[26,27] In GO water-isopropanol dispersion, water molecules prefer to be trapped around GO sheets due to the lower intercalation energy compared with isopropanol. As shown in Figure 3c, because of the limited fraction of water, GO sheets are further concentrated around water molecule to maintain a stable dispersion, which induces microphase separation between water and isopropanol molecules, forming micro liquid-liquid interfaces around the GO sheets clusters. These interfaces allow r-GO sheets gradually precipitated and assembled into the connected framework. The separated water molecules are trapped inside the network and serve as spacers to avoid parallel restacking, forming an integral hydrogel. The phase separation and concentrated water phase can be further confirmed through the nuclear magnetic resonance (NMR) measurement. As shown in Figure 3d, the liquid inside hydrogel had a stronger water peak compared with outside, demonstrating the water was mainly accumulated inside the hydrogel. The UV-Vis spectra (Figure S12, Supporting Information) also observed the similar solvent gradient, where the intensity of the isopropanol outside hydrogel was increased after solvothermal treatment. Above results effectively support our hypothesis that the hydrated GO sheets trapped water molecules as spacers during the reduction process, inducing microphase separation and providing more liquid-liquid interfaces facilitated the r-GO assembly process.

The above discussion demonstrates the water acts as a spacer in gelation and its fraction would influence r-GO microstructure. Therefore, more characterization about water fraction was further investigated in detail. Photos in Figure 4a show that the freeze-dried r-GO aerogels with different water fraction (10 to 40 vol%) were synthesized at the same GO concentration (0.4 mg mL^{-1}). The volume of the r-GO aerogels and voids in microstructure (SEM images in Figure S13, Supporting Information) were gradually increased with higher water fraction but the density was kept decreasing, indicating the water serves as soft templates and facilitates the formation of the porous framework. The N_2 adsorption measurement in Figure 4b shows that r-GO aerogels have hierarchical porous structure and gradually increased specific surface areas (SSAs; $335\text{--}564 \text{ m}^2 \text{ g}^{-1}$) and pore volumes ($0.33\text{--}0.67 \text{ cm}^3 \text{ g}^{-1}$). The more developed porous structure also presents lower resistance and higher ion diffusion in electrochemical impedance spectroscopy (EIS) profile (Figure 4c). These results further indicated the water was performed as a spacer and manipulated the microstructures of hydrogels. As expected, no hydrogel is formed when the water fraction is higher than 50 vol%, since too much water induces less interaction between GO sheets.

The gelation in a larger water fraction requires a higher GO concentration. Therefore, 2 mg mL^{-1} GO solution was used to synthesize hydrogels in pure water and water-isopropanol mixture (40 vol% water) to characterize the structure difference. The hydrogel formed in pure water exhibits a more developed hierarchical pore structure (Figure 4d) and a much higher SSA ($530 \text{ m}^2 \text{ g}^{-1}$) compared with the hydrogel obtained

in the mixture ($321 \text{ m}^2 \text{ g}^{-1}$). These results are in good agreement with the previous discussion that water performed as a spacer and promoted a more developed porous structure. Figure S14 in the Supporting Information shows the r-GO aerogels obtained from different GO concentration, even at a concentration as low as 0.1 mg mL^{-1} , an integral aerogel can still be formed. Although higher GO concentration induces larger volume of hydrogels, pore structures are similar except for a slight decrease in SSA (Figure S15, Supporting Information), which may be ascribed to the partial overlap of r-GO sheets. The hydrogels obtained at relatively high concentrations are hard to avoid the restacking or aggregation of r-GO sheets, which lowers the effective utilization of r-GO surface area and electrochemical performance. Therefore, the GO gelation at lower concentrations is recommended to avoid restacking and ensure the sufficient utilization of individual r-GO sheets. Note that 0.1 mg mL^{-1} is the lowest GO concentration of gelation in this work because experiments with lower GO concentrations are difficult to precisely control and limited for observation.

In conclusion, the gelation of GO at an ultralow concentration has been realized with artificial microinterfaces in a water–isopropanol mixture. Due to the different intercalation energies between GO sheets and solvents, GO sheets prefer to be surrounded by water molecules compared with isopropanol. Microphase separation induces the formation of liquid–liquid interfaces, where r-GO sheets are concentrated and assembled into the interconnected framework. Both experimental and simulation results demonstrate that the higher attraction between GO sheets and water, leading the water act as a spacer to facilitate the gelation and control its microstructures. Such a gelation process provides a feasible approach to assemble GO at ultralow concentrations and to tune the structure of GO hydrogels for different applications, which also provides a better understanding of the mechanism of GO gelation.

Experimental Section

Sample Preparation: Graphite oxide was prepared from graphite powder by the modified Hummers method, and then, GO aqueous dispersion was obtained under high power ultra-sonication (JY92-N, 160W) for 2 h. This dispersion was mixed with isopropanol with different fractions under sonication to form the uniform and stable dispersion. Then, 35 mL dispersion was sealed in a 50 mL Teflon-lined autoclave and solvothermal at 200°C for 6 h, and after the autoclave cooled down, a black cylindrical hydrogel was obtained. The hydrogel was immersed in the deionized water for 24 h to exchange the residual isopropanol. Finally, the graphene hydrogel was quenched in the liquid nitrogen and then freeze-dried.

Characterization: The morphology of samples was characterized by SEM (Hitachi, S-4800, Japan). AFM image was obtained on Dimension Icon (ScanAsyst, Bruker). Raman spectra were recorded using a multi-wavelength micro-Raman spectroscopy (JY HR800) utilizing 532 nm incident radiation. FT-IT spectra were measured by Thermo Scientific (Nicolet iS50). UV spectra were collected by UV–vis–NIR (near-infrared) systems (Cary 5000). Zeta potentials were characterized by Malvern Zetasizer. ^1H NMR spectra were determined on a Bruker AVANCE DMX III 400M. The rheological properties were measured with the HAAKE MARS III rheometer (Thermo Scientific, Karlsruhe, Germany). The r-GO hydrogel was prepared from 0.8 mg mL^{-1} GO solution in pure water through hydrothermal treatment and the r-GO suspension was obtained from 0.5 mg mL^{-1} GO aqueous solution. Nitrogen adsorption

experiments were conducted at 77 K using BEL mini-instrument and the specific surface area was obtained by Brunauer–Emmett–Teller analyses of the adsorption isotherms.

Electrochemical Measurements: The electrochemical experiments were carried out using a three-electrode system with an aqueous system (electrolyte: 6 M KOH solution). The working electrode, composed of 90 wt% r-GO and 10 wt% polytetrafluoroethylene binder, was posted on the Ni-foam current electrode, platinum plate, and Ag/AgCl electrode as the counter and reference electrodes. The EIS was measured by Solartron 1470E CellTest electrochemical workstation. The EIS plots were obtained in the frequency range from 100 kHz to 10 mHz at an open-circuit potential.

Computational Details: First-principles calculations were performed using DFT method implemented in the Vienna ab initio simulation package.^[28] The ion–electron interactions were treated with the projected augmented wave pseudopotentials,^[29] and the general gradient approximation parameterized by Perdew, Burke, and Ernzerhof was used to describe the exchange–correlation potential.^[30] The plane-wave basis was expanded up to a cutoff energy of 615 eV. All structures were optimized by a conjugate gradient method until the force component on every atom was less than $0.02 \text{ eV } \text{\AA}^{-1}$. In addition, the Tkatchenko–Scheffler (DFT-TS) method was used to include the van der Waals interactions in the system.^[31] The interlayer distance of graphite was calculated to test the validity of DFT-TS method in this study system. The calculated result was 3.350 Å, which was very close to the value of 3.354 Å reported by Zhao et al. in the experiment,^[32] indicating an accurate calculation of long-range van der Waals interactions in DFT-TS method.

A DLG for the intercalation of water and isopropanol molecule and full relaxed all atoms was adopted. The vacuum layer, which was larger than 20 Å, was used to make sure that there was no interaction between different slabs. A supercell of DLG composed of 5×5 repeating unit cells (the length of supercell along the in-plane direction of graphene of about 12 Å) was used to avoid the interaction of neighboring intercalated molecule. The k-point mesh used for the calculation was $5 \times 5 \times 1$. A larger cell or more k-points were tested to yield the same results in test calculations.

Supporting Information

Supporting Information is available from the Wiley Online Library or from the author.

Acknowledgements

The authors appreciate the support from the National Science Fund for Distinguished Young Scholars, China (No. 51525204), National Natural Science Foundation of China (Nos. 51772164, 11874036, and U1601206), Guangdong Natural Science Funds for Distinguished Young Scholar (2017B030306006), and Shenzhen Basic Research Projects (Nos. JCYJ20170412171359175 and JCYJ20170412171630020) and Local Innovative and Research Teams Project of Guangdong Pearl River Talents Program (2017BT01N111).

Conflict of Interest

The authors declare no conflict of interest.

Keywords

assembly, gelation, graphene oxide, interface, isopropanol

Received: August 4, 2018

Revised: December 6, 2018

Published online: December 28, 2018

- [1] J. Kim, L. J. Cote, F. Kim, W. Yuan, K. R. Shull, J. X. Huang, *J. Am. Chem. Soc.* **2010**, 132, 8180.
- [2] D. Li, M. B. Muller, S. Gilje, R. B. Kaner, G. G. Wallace, *Nat. Nanotechnol.* **2008**, 3, 101.
- [3] W. Lv, C. Zhang, Z. J. Li, Q. H. Yang, *J. Phys. Chem. Lett.* **2015**, 6, 658.
- [4] J. J. Shao, W. Lv, Q. H. Yang, *Adv. Mater.* **2014**, 26, 5586.
- [5] S. H. Lee, D. H. Lee, W. J. Lee, S. O. Kim, *Adv. Funct. Mater.* **2011**, 21, 1338.
- [6] S. H. Lee, H. W. Kim, J. O. Hwang, W. J. Lee, J. Kwon, C. W. Bielawski, R. S. Ruoff, S. O. Kim, *Angew. Chem.* **2010**, 122, 10282.
- [7] L. Qiu, J. Z. Liu, S. L. Chang, Y. Wu, D. Li, *Nat. Commun.* **2012**, 3, 1241.
- [8] M. A. Worsley, P. J. Pauzauskie, T. Y. Olson, J. Biener, J. H. Satcher Jr., T. F. Baumann, *J. Am. Chem. Soc.* **2010**, 132, 14067.
- [9] Z. S. Wu, Y. Sun, Y. Z. Tan, S. B. Yang, X. L. Feng, K. Mullen, *J. Am. Chem. Soc.* **2012**, 134, 19532.
- [10] F. Yavari, Z. P. Chen, A. V. Thomas, W. C. Ren, H. M. Cheng, N. Koratkar, *Sci. Rep.* **2011**, 1, 166.
- [11] X.-C. Dong, H. Xu, X.-W. Wang, Y.-X. Huang, M. B. Chan-Park, H. Zhang, L.-H. Wang, W. Huang, P. Chen, *ACS Nano* **2012**, 6, 3206.
- [12] J. Wang, G. Chen, Z. Zhao, L. Sun, M. Zou, J. Ren, Y. Zhao, *Sci. China Mater.* **2018**, 61, 1314.
- [13] U. N. Maiti, J. Lim, K. E. Lee, W. J. Lee, S. O. Kim, *Adv. Mater.* **2014**, 26, 615.
- [14] J. Lim, G. Y. Lee, H. J. Lee, S. K. Cha, D. S. Choi, S. H. Koo, W. J. Lee, S. O. Kim, *Energy Storage Mater.* **2019**, 16, 251.
- [15] Y. Xu, G. Shi, X. Duan, *Acc. Chem. Res.* **2015**, 48, 1666.
- [16] Y. Xu, K. Sheng, C. Li, G. Shi, *ACS Nano* **2010**, 4, 4324.
- [17] Y. Tao, X. Xie, W. Lv, D.-M. Tang, D. Kong, Z. Huang, H. Nishihara, T. Ishii, B. Li, D. Golberg, *Sci. Rep.* **2013**, 3, 2975.
- [18] Y. Li, J. Chen, L. Huang, C. Li, J. D. Hong, G. Shi, *Adv. Mater.* **2014**, 26, 4789.
- [19] K. Hu, X. Xie, T. Szkopek, M. Cerruti, *Chem. Mater.* **2016**, 28, 1756.
- [20] H. Wang, J. T. Robinson, X. Li, H. Dai, *J. Am. Chem. Soc.* **2009**, 131, 9910.
- [21] S. Dubin, S. Gilje, K. Wang, V. C. Tung, K. Cha, A. S. Hall, J. Farrar, R. Varshneya, Y. Yang, R. B. Kaner, *ACS Nano* **2010**, 4, 3845.
- [22] G. Wang, L.-T. Jia, B. Hou, D.-B. Li, J.-G. Wang, Y.-H. Sun, *New Carbon Mater.* **2015**, 30, 30.
- [23] S. Stankovich, D. A. Dikin, R. D. Piner, K. A. Kohlhaas, A. Kleinhammes, Y. Jia, Y. Wu, S. T. Nguyen, R. S. Ruoff, *Carbon* **2007**, 45, 1558.
- [24] Y. Yoon, K. Lee, C. Baik, H. Yoo, M. Min, Y. Park, S. M. Lee, H. Lee, *Adv. Mater.* **2013**, 25, 4437.
- [25] C. Mattevi, G. Eda, S. Agnoli, S. Miller, K. A. Mkhoyan, O. Celik, D. Mastrogianni, G. Granozzi, E. Garfunkel, M. Chhowalla, *Adv. Funct. Mater.* **2009**, 19, 2577.
- [26] S. Dixit, J. Crain, W. Poon, J. Finney, A. Soper, *Nature* **2002**, 416, 829.
- [27] U. Halim, C. R. Zheng, Y. Chen, Z. Lin, S. Jiang, R. Cheng, Y. Huang, X. Duan, *Nat. Commun.* **2013**, 4, 2213.
- [28] G. Kresse, J. Furthmüller, *Phys. Rev. B* **1996**, 54, 11169.
- [29] P. E. Blochl, *Phys. Rev. B* **1994**, 50, 17953.
- [30] J. P. Perdew, K. Burke, M. Ernzerhof, *Phys. Rev. Lett.* **1996**, 77, 3865.
- [31] A. Tkatchenko, M. Scheffler, *Phys. Rev. Lett.* **2009**, 102, 073005.
- [32] Y. X. Zhao, I. L. Spain, *Phys. Rev. B* **1989**, 40, 993.